Eur Biophys J (2012) 41:475–482
DOI 10.1007/s00249-012-0801-0

ORIGINAL PAPER

EBSA
Biophysics in Europe

Comparative analysis of the orientation of transmembrane peptides using solid-state ^{2}H- and ^{15}N-NMR: mobility matters

Stephan L. Grage · Erik Strandberg · Parvesh Wadhwani · Santiago Esteban-Martín · Jesús Salgado · Anne S. Ulrich

Received: 14 December 2011 / Revised: 23 February 2012 / Accepted: 6 March 2012 / Published online: 28 March 2012

Abstract Many solid-state nuclear magnetic resonance (NMR) approaches for membrane proteins rely on orientation-dependent parameters, from which the alignment of peptide segments in the lipid bilayer can be calculated. Molecules embedded in liquid-crystalline membranes, such as monomeric helices, are highly mobile, leading to partial averaging of the measured NMR parameters. These dynamic effects need to be taken into account to avoid misinterpretation of NMR data. Here, we compare two common NMR approaches: ^{2}H-NMR quadrupolar waves, and separated local field ^{15}N–^{1}H polarization inversion spin exchange at magic angle (PISEMA) spectra, in order to identify their strengths and drawbacks for correctly determining the orientation and mobility of α-helical transmembrane peptides. We first analyzed the model peptide WLP23 in oriented dimyristoylphosphatidylcholine (DMPC) membranes and then contrasted it with published data on GWALP23 in dilauroylphosphatidylcholine (DLPC). We only obtained consistent tilt angles from the two methods when taking dynamics into account. Interestingly, the two related peptides differ fundamentally in their mobility. Although both helices adopt the same tilt in their respective bilayers (~20°), WLP23 undergoes extensive fluctuations in its azimuthal rotation angle, whereas GWALP23 is much less dynamic. Both alternative NMR methods are suitable for characterizing orientation and dynamics, yet they can be optimally used to address different aspects. PISEMA spectra immediately reveal the presence of large-amplitude rotational fluctuations, which are not directly seen by ^{2}H-NMR. On the other hand, PISEMA was unable to define the azimuthal rotation angle in the case of the highly dynamic WLP23, though the helix tilt could still be determined, irrespective of any dynamics parameters.

Keywords Membrane peptide orientation and dynamics · WALP family peptides · Geometric analysis of labeled alanines (GALA) · ^{15}N–^{1}H PISEMA · Models of peptide dynamics · Selective isotope labeling

Electronic supplementary material The online version of this article (doi:10.1007/s00249-012-0801-0) contains supplementary material, which is available to authorized users.

S. L. Grage · E. Strandberg · P. Wadhwani · A. S. Ulrich (✉)
Institute for Biological Interfaces (IBG-2) and Institute of Organic Chemistry and CFN, Karlsruhe Institute of Technology, P.O. Box 3640, 76021 Karlsruhe, Germany
e-mail: anne.ulrich@kit.edu

S. Esteban-Martín
Joint BSC-IRB Research Programme in Computational Biology, Institute for Research in Biomedicine (IRB Barcelona), Parc Científic de Barcelona, Baldiri Reixac 10, 08028 Barcelona, Spain

J. Salgado
Institute of Molecular Science, University of Valencia, 46980 Paterna (Valencia), Spain

Introduction

The orientation of peptides in lipid bilayers gives important clues on their structure–function relationship. For example, analysis of peptide orientation has been used to explain pore formation (Strandberg et al. 2009a) and to study the response of transmembrane helices to hydrophobic mismatch (Strandberg et al. 2004, 2012; van der Wel et al. 2002). Apart from a few examples of ^{13}C-NMR (e.g., Cornell et al. 1988), two related solid-state NMR approaches are typically employed to determine peptide alignment in oriented bilayer samples: either orientation-dependent

^{2}H-NMR quadrupolar splittings are analyzed by the so-called geometric analysis of labeled alanines (GALA) approach (van der Wel et al. 2002), or PISEMA-type experiments are used to obtain ^{15}N chemical shifts correlated with ^{1}H–^{15}N dipolar couplings in the polarity index slant angle (PISA) approach (Marassi and Opella 2000; Nevzorov and Opella 2007; Wang et al. 2000; Wu et al. 1994). In both cases, the peptide helix is treated as a rigid body which is tilted away from the membrane normal by an angle τ and rotated around its long axis by an azimuthal angle ρ. The helix orientation in terms of τ and ρ is calculated by comparing experimental ^{2}H-NMR splittings or PISEMA observables from different labeled sites on the molecule with predicted values in a root–mean-square deviation (rmsd) analysis.

A potential drawback of these NMR methods is the fact that peptide dynamics can have a strong influence on the observed NMR parameters, which may affect the results of the analysis. Such dynamics can in principle be avoided if measurements are performed at low temperature (Smith et al. 1994). However, peptide orientation tends to change dramatically with the temperature and phase state of the membrane (Afonin et al. 2008; Grage et al. 2010), hence structures should be determined at the temperature of biological relevance. For example, molecular dynamics (MD) simulations suggest that membrane-embedded model transmembrane peptides (WALP23 and WLP23) show broad distributions of ρ angles, with width (standard deviation) σ_ρ of 60–90°. Pronounced mobility will lead to considerable averaging of the corresponding ^{2}H-NMR splittings. It has been demonstrated that such fluctuations can even obscure the peptide tilt angle when they are not taken into account properly (Esteban-Martín and Salgado 2007; Özdirekcan et al. 2007). However, it has been argued that GALA and PISA are affected by dynamics in different ways, because the principal axes of the respective interaction tensors are oriented in different ways within the molecular frame (Esteban-Martín et al. 2009a, 2010; Strandberg et al. 2009b). Namely, the NMR observables in a PISEMA spectrum depend on the orientation of the N–H bond direction, which is aligned almost parallel to the helix axis. As a consequence, the center of the PISA wheel depends only on the peptide tilt, but not on the helix rocking motion, which rather affects the size of the wheel (Esteban-Martín et al. 2009a). In contrast, in the case of GALA, the relevant interaction tensor is given by the C_α–C_β bond, thus pointing away from the helix axis by about 60°, a value that is close to the magic angle. With this geometry, the helix orientation and dynamics are more entangled for ^{2}H-splittings (Esteban-Martín et al. 2010; Strandberg et al. 2009b).

In several recent approaches, peptide dynamics has been duly considered in ^{2}H-NMR analyses, e.g., by implementing time-averaged Gaussian distributions of the orientation angles (Strandberg et al. 2009b), by obtaining distributions of peptide orientation angles with the help of MD simulations (Kim et al. 2011; Monticelli et al. 2010) or free energy calculations (Esteban-Martín et al. 2009b), or by simultaneously fitting ^{2}H-, ^{13}C-, and ^{15}N-NMR data (Holt et al. 2010; Separovic et al. 1993). Likewise, the influence of dynamics on PISEMA spectra (Jo and Im 2011) and ^{2}H quadrupolar splittings (Kim et al. 2011) has been considered using ensemble-restrained MD simulations.

Here, we report PISEMA data and analysis of a specifically ^{15}N-labeled peptide WLP23 (acetyl-$GW_2L_{17}W_2$A-amide). This transmembrane model helix has been described by MD simulations to be highly mobile when reconstituted in oriented DMPC membranes (Esteban-Martín and Salgado 2007). A set of ^{2}H-NMR splittings is already available from the literature, allowing direct comparison with our ^{15}N-NMR data (Özdirekcan et al. 2005). It was thus possible to subject both the old ^{2}H-NMR and the new PISEMA data to proper structural analysis including dynamic effects. We used the same backbone structure and the same model for dynamics, namely an averaged Gaussian distribution of ρ, mimicking a rocking motion around the helix axis (Esteban-Martín and Salgado 2007; Esteban-Martín et al. 2009a, 2010; Strandberg et al. 2009b) [see "Materials and methods" for details on the structure, dynamic-PISA (*dyn*-PISA) and dynamic-GALA (*dyn*-GALA) models, and error analysis]. To provide another example for comparison with this highly mobile WLP23 peptide, we also present here the PISEMA and GALA analysis of the less dynamic peptide GWALP23 [acetyl-GGALW(LA)$_6$LWLAGA-ethanolamide, in DLPC], for which we have re-analyzed the published experimental data (Vostrikov et al. 2008) using the same procedure as for WLP23.

Materials and methods

Materials

Dimyristoylphosphatidylcholine (DMPC) was purchased from Avanti Polar Lipids (Alabaster, AL). Fmoc-protected amino acids and coupling reagents used for peptide synthesis were purchased from Iris Biotech GmbH (Marktredwitz, Germany) or Novabiochem (Merck Chemicals Ltd., Nottingham, UK) and were used without any further purification. Solvents for synthesis and purification were purchased from Acros Organics (Geel, Belgium) or Biosolve (Valkenswaard, The Netherlands). Ultraviolet (UV)-grade chloroform and methanol used for NMR sample preparation were obtained from VWR international (Bruchsal, Germany).

Sample preparation

WLP23 with the sequence (Ac-GW_2L_5-$\boldsymbol{L}_7$-L_5W_2A-amide) was synthesized with seven ^{15}N-labeled leucines (^{15}N-Leu) in the central stretch (positions 9–15) of the peptide as shown in italics. WLP23 was synthesized on an automated peptide synthesizer (ABI 433A, Applied Biosystems) at 100 μmolar scale by following Fmoc solid-phase synthesis protocols as previously described by Killian et al. (1996). ^{15}N-Leu was coupled by using 2.0 equivalents excess of Fmoc-^{15}N-Leu in presence of 1-benzo-triazol-1-yl-*N*,*N*,*N*′,*N*′-tetramethyluronium hexafluorophosphate (HBTU) and 1-hydroxybenzotriazole (HOBT) in dimethylformamide (DMF) in presence of *N*,*N*-diisopropylethylamine (DIEA). The crude peptides were treated as described previously (Killian et al. 1996) after an initial treatment over a desalting column to remove the excess reagents from the cleavage step. Several fractions were collected, and the desired product was characterized using mass spectrometry, where besides the expected peptide mass no other products were detected.

Oriented NMR samples were prepared by co-dissolving lipid and peptide in suitable organic solvents, spreading the mixture on glass plates, removal of the organic solvent, and subsequent hydration. Our initial attempts to prepare NMR samples using hexafluoroisopropanol to solubilize the hydrophobic peptide and chloroform to dissolve lipids resulted in a clear solution which upon drying/hydration gave an oily film with very low degree of lipid orientation. An optimized sample preparation method was subsequently used for all measurements. WLP23 (2.3 mg) was suspended in chloroform (100 μl) to which methanol (50 μl) was added to obtain a clear solution. DMPC (18.8 mg) was dissolved in chloroform:methanol (10:3 v/v) and was added to the peptide solution to obtain a peptide:lipid ratio of 1:40. The resulting clear solution was uniformly spread over 18 glass plates of size 7.5 mm × 9 mm × 0.08 mm (Marienfeld Laboratory Glassware, Lauda-Königshofen, Germany). Organic solvent was removed under vacuum, and the glass plates were stacked and hydrated for 18 h at 48 °C in a chamber with humidity created from saturated solution of K_2SO_4. The stack was placed in a custom-made glass vessel (New Era) together with wet paper to keep the sample fully hydrated, and sealed with parafilm.

Solid-state ^{15}N-NMR experiments

SAMPI4 experiments (Nevzorov and Opella 2007) correlating the ^{15}N chemical shift and ^{1}H–^{15}N dipolar coupling were performed at 40 °C on an Avance III Bruker NMR spectrometer (Bruker Biospin, Karlsruhe, Germany) equipped with a wide-bore 500-MHz (^{1}H resonance frequency) magnet. The spectra were acquired using a double-tuned probe with a low-E flat-coil resonator (3 mm × 9 mm cross-section), employing a ^{1}H and ^{15}N radiofrequency (rf) field strength of 51 kHz during the cross-polarization and indirect dimension of the two-dimensional (2D) experiment, and 30 kHz ^{1}H SPINAL64 decoupling during acquisition. Acquisition times were 3.5 ms in the indirect dimension (^{1}H–^{15}N dipolar coupling) and 10 ms in the direct dimension (^{15}N chemical shift). A recycle time of 8 s was used in the ^{15}N-NMR experiments.

Fitting procedures

To fit the data, ^{2}H quadrupolar splittings, ^{1}H–^{15}N dipolar splitting, and ^{15}N chemical shifts were calculated for different peptide alignments specified by tilt angle τ, mean azimuthal rotation ρ_0, and a parameter describing rocking motions around the helix axis, σ_ρ, as given by Strandberg et al. (2009b). To achieve dynamically averaged NMR parameters, each parameter was calculated for a Gaussian distribution of ρ angles, with mean ρ_0 and standard deviation σ_ρ, and averaged over this distribution. In the case of GALA, the root-mean-square deviation between the experimental splittings $\Delta_{\mathrm{exp},k}$ and the calculated splittings $\Delta_{\mathrm{cal},k}$ of the N labeled sites was characterized by $\mathrm{rmsd}_{\mathrm{GALA}}$, defined as

$$\mathrm{rmsd}_{\mathrm{GALA}} = \left[\sum_k \left(\Delta_{\mathrm{exp},k} - \Delta_{\mathrm{cal},k}\right)^2 / N\right]^{1/2}.$$

In the PISA case, the first moment M_{1X} and second moment M_{2X} of the distribution of both the ^{15}N chemical shift ($X = \mathrm{CS}$) and ^{1}H–^{15}N dipolar couplings ($X = \mathrm{DD}$) were used to characterize the 2D spectrum:

$$M_{1X} = \sum_k I_k \delta_{X,k} / \sum_k I_k,$$

$$M_{2X} = \sum_k I_k \left(\delta_{X,k} - M_{1X}\right)^2 / \sum_k I_k,$$

where the sums are over all points in the spectrum, I_k is the intensity in point k, and $\delta_{X,k}$ is the respective ^{15}N chemical shift ($X = \mathrm{CS}$) or ^{1}H–^{15}N dipolar coupling ($X = \mathrm{DD}$). The center of the distribution is characterized by the first moments, whereas the second moments quantify the width of the signal intensity distribution. $\mathrm{rmsd}_{\mathrm{PISA}}$ was calculated from these moments as

$$\begin{aligned}\mathrm{rmsd}_{\mathrm{PISA}} = \Big[& a_1 \left(\left(M_{1\mathrm{CS,exp}} - M_{1\mathrm{CS,cal}}\right)/d_{\mathrm{CS}}\right)^2 \\ & + a_1 \left(\left(M_{1\mathrm{DD,exp}} - M_{1\mathrm{DD,cal}}\right)/d_{\mathrm{DD}}\right)^2 \\ & + a_2 \left(\left(M_{2\mathrm{CS,exp}}^{1/2} - M_{2\mathrm{CS,cal}}^{1/2}\right)/M_{2\mathrm{CS,cal}}^{1/2}\right)^2 \\ & + a_2 \left(\left(M_{2\mathrm{DD,exp}}^{1/2} - M_{2\mathrm{DD,cal}}^{1/2}\right)/M_{2\mathrm{DD,cal}}^{1/2}\right)^2 \Big]^{1/2}.\end{aligned}$$

a_1 and a_2 weigh the contributions from the first or second moments. When using only the center of the PISA wheel,

Table 1 Influence of different CSA or dipolar coupling values on the best fit values of τ and σ_ρ in the analysis of PISEMA NMR data

	Values used in the analysis			Reduced ^{15}N CSA span			Increased dipolar coupling		
^{15}N CSA	56 ppm, 91 ppm, 230 ppm			59.6 ppm, 92.7 ppm, 224.8 ppm			56 ppm, 91 ppm, 230 ppm		
^{1}H–^{15}N coupling (max. splitting)	20.0 kHz			20.0 kHz			21.0 kHz		
	τ/°	σ_ρ/°	rmsd	τ/°	σ_ρ/°	rmsd	τ/°	σ_ρ/°	rmsd
WLP23: PISA	21	107	0.007	21	106	0.016	22	111	0.012
GWALP23: PISA	20	78	0.042	19	76	0.061	22	84	0.054

$a_1 = 1/2$ and $a_2 = 0$; when using both center and width, $a_1 = 1/4$ and $a_2 = 1/4$. $d_{CS} = 174$ ppm and $d_{DD} = 15$ kHz are the spans of the chemical shift and dipolar interaction tensor, respectively.

A quadrupolar constant was used which would result in a splitting of 74 kHz for the CD_3-group of an immobilized peptide with the C_α–C_β bond of the labeled alanine pointing along the magnetic field (Strandberg et al. 2009b). This value, which was measured in a dry powder of the antimicrobial peptide PGLa, is slightly reduced compared with the value of 83.5 kHz expected for a CD_3-group because of internal side-chain motions. The orientation of the C_α–C_β direction with respect to the helix is described by the angles $\varepsilon_{\|} = 58.9°$ and $\varepsilon_{\perp} = -53.2°$, using the conventions from previous WALP publications (Strandberg et al. 2004; van der Wel et al. 2002). A ^{1}H–^{15}N dipolar coupling resulting in a maximum splitting of 20 kHz (Walther et al. 2010), and a ^{15}N tensor with principal values of 56, 91, and 230 ppm, was used (Lee et al. 2001) in the PISA analysis. The principal axis corresponding to the largest tensor component was assumed to be turned away from the N–H bond by 18.5°, and an α-helix with torsion angles of $\varphi = -60.7°$ and $\psi = -44.7°$, and a helix pitch of 100° was assumed in the calculations (Walther et al. 2010). For each peptide used here, a pdb structure meeting the above helix geometry is deposited in the supplementary material.

Error estimate

Judging from whether the rmsd is within experimental error, errors for τ and σ_ρ can be estimated in the case of GALA from rmsd plots, as shown in Fig. 2. From experience, ^{2}H quadrupolar splitting can be reproduced within approximately 1 kHz. Assuming 1 kHz experimental uncertainty, the error of the tilt angle τ is approximately 5°, and the uncertainty of σ_ρ is in the range 15–30°. A similar estimate for PISA is not possible due to the lack of resolved individual peaks in the ^{15}N PISEMA spectra.

Besides statistical errors, uncertainties in the assumptions made in the models used for fitting, e.g., the ^{15}N chemical shift tensor values or ^{1}H–^{15}N dipolar coupling, contribute to the error of τ and σ_ρ. To assess how the interaction tensors influence the obtained peptide alignment, the PISEMA data were fitted using a ^{15}N chemical shift tensor with 5 % smaller span (59.6, 92.7, and 224.8 ppm), or using a 5 % increased dipolar coupling. The results are summarized in Table 1 and indicate a small dependence on the tensor values, resulting in uncertainty of 1–2° in τ and 3–5° in σ_ρ.

Results and discussion

The PISEMA spectrum of WLP23 in DMPC, labeled with ^{15}N in seven sites (positions 9–15), is shown in Fig. 1a. Instead of seven resolved resonances, it exhibits a single broad peak that lies on the trajectory along which the center of PISA wheels is expected to move with varying tilt angle (dotted blue straight line, Fig. 1a). Considering that mosaic spread might contribute to the residual width intensity distribution, the actual spread could be even smaller. The observed collapse in the intensity distribution, instead of observing a resolved PISA wheel, suggests that large-amplitude fluctuations must be present in ρ (Esteban-Martín et al. 2009a). This hinders specific assignment of resonances and prevents determination of ρ. We therefore focus here on the tilt angle τ and on the standard deviation of the ρ distribution, σ_ρ, which describes the extent of rotational fluctuations. (Note, however, that ρ angles can be obtained from the GALA analysis; see below and Table 2.) If we first consider a static peptide (by fixing $\sigma_\rho = 0$), we obtain a rather large PISA wheel (black solid wheel, Fig. 1a). It corresponds to $\tau = 21°$, and its center coincides with that of the experimental broad peak (Table 2). Next, we allow both the center and the size of the PISA wheels to be varied in the rmsd calculation of the static case. The resulting best-fit wheel is much displaced from the experimental signal (black dotted wheel, Fig. 1a). It is clearly impossible to match both the center and the size of the wheel at the same time, when using a static model for data analysis. On the other hand, when fitting with the dynamic

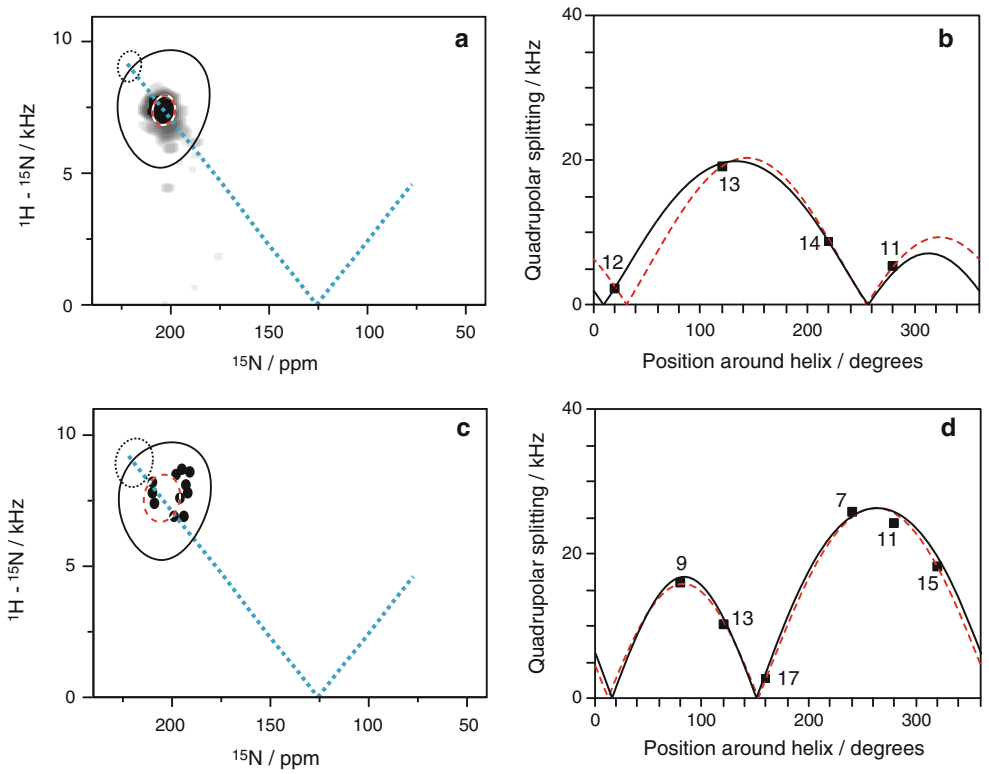

Fig. 1 Experimental ^{15}N/^{1}H–^{15}N PISEMA spectrum of WLP23 in DMPC, labeled with ^{15}N in positions 9–15 (**a**). ^{2}H quadrupolar splittings of WLP23 labeled in positions 11–14, taken from Özdirekcan et al. (2005) (**b**). Reconstructed PISEMA peaks (**c**) and ^{2}H quadrupolar splittings of GWALP23 in DLPC (**d**), taken from Vostrikov et al. (2008). The straight *blue dotted lines* in the PISEMA spectra (**a**, **c**) represent the expected trajectory of PISA wheels as a function of τ. Best-fit calculated wheels matching the experimental centers of intensities (**a**, **c**) and quadrupolar waves (**b**, **d**) using the static models are shown as *black solid lines*. Best-fit wheels considering both center and width as first and second moments of the intensity distribution, obtained using a static model, are depicted as *black dotted lines* (**a**, **c**). Best fits based on dynamical ρ-distribution models (*dyn*-PISA in **a**, **c**, or *dyn*-GALA in **b**, **d**) are shown as *red dashed* wheels or waves. In the static model, a single, uniform helix orientation is assumed given by a tilt angle τ and azimuthal rotation ρ. In the dynamic model, a single value is assumed for τ, but a Gaussian distribution is assumed for ρ, of which the time average is observed

Table 2 Best-fit tilt angle (τ), and extent of azimuthal fluctuations (σ_ρ), as obtained with either static or dynamic implementations in the PISA and GALA analyses

	Static		Dynamic (ρ-distribution)		
	τ/°	ρ/°	τ/°	ρ/°	σ_ρ/°
WLP23: PISA	21	n.a.	21	n.a.	107
WLP23: GALA	8	176	24	186	80
GWALP23: PISA	21	n.a.	20	n.a.	78
GWALP23: GALA	13	306	18	305	46

For rmsd values and error estimates see Table 1

model (*dyn*-PISA, allowing $\sigma_\rho \neq 0$), we obtain very good agreement with the experimental data (in terms of both center and size of the wheel, red dashed wheel, Fig. 1a), for $\tau = 21°$ and $\sigma_\rho = 107°$. These findings demonstrate that the tilt angle determined by the center of the PISA wheel, which is essentially independent of dynamics in the PISEMA analysis, can be considered a safe result even in the absence of spectral resolution. However, only the dynamic analysis is capable of giving also an estimate of the amplitude of helix rotational fluctuations. The large value of σ_ρ observed here describes a wide spread of the azimuthal rotation angle, suggesting a highly dynamic peptide, just as predicted by MD simulations (Esteban-Martín and Salgado 2007).

The ^{2}H quadrupolar splittings obtained for the same peptide WLP23 by Özdirekcan et al. (2005) are shown in Fig. 1b, together with helical waves fitted here using our static and dynamic GALA models. Although the fit with the static model is good (Fig. 1b, black solid line, rmsd = 0.50 kHz), *dyn*-GALA gives a better result (Fig. 1b, red dashed line, rmsd = 0.06 kHz). Most importantly, however, while a tilt angle of 8° was obtained by static GALA, *dyn*-GALA leads to a much larger value of $\tau = 24°$. Clearly, only the latter tilt is compatible with the result of the PISA analysis above ($\tau = 21°$), which as we had explained can be considered a safe result. It also matches the expected tilt angle by which the peptide can ideally avoid hydrophobic mismatch between the hydrophobic length of the helix and the effective membrane thickness (Strandberg et al. 2012). Furthermore,

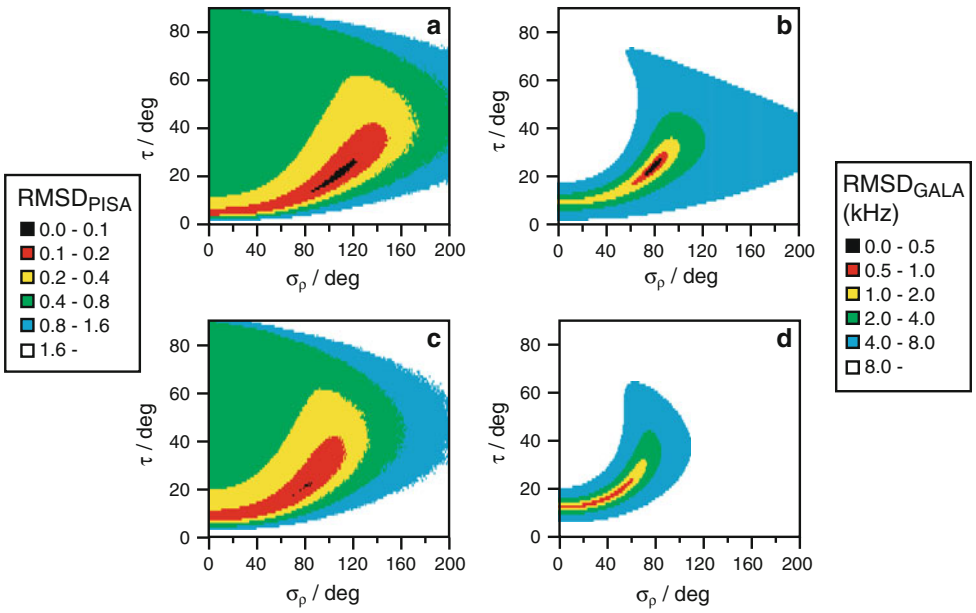

Fig. 2 Differences of calculated and experimental PISEMA spectra of WLP23 (**a**), ^{2}H-NMR spectra of WLP23 (**b**), PISEMA spectra of GWALP23 (**c**), and ^{2}H-NMR spectra of GWALP23 (**d**) as a function of the tilt angle τ and the extent of ρ-fluctuations, σ_ρ. PISEMA spectra were compared using the root-mean-square deviation of the first and second moments of the spectra, as described in the "Materials and methods" section. The ^{15}N-NMR values of GWALP23 were taken from Vostrikov et al. (2008). The ^{2}H-NMR data was compared by means of the root-mean-square deviation of calculated and experimental ^{2}H quadrupolar splittings of selectively labeled positions, taken from Özdirekcan et al. (2005) and Vostrikov et al. (2008) in the case of WLP23 and GWALP23, respectively

this value approaches the averaged tilt ($\sim$30°) of distributions obtained from different types of MD simulations (Esteban-Martín and Salgado 2007; Im and Brooks 2005; Özdirekcan et al. 2007) and free energy calculations (Esteban-Martín et al. 2009b). The critical need for proper dynamical analysis has thus been demonstrated once more, as already pointed out in previous studies on a similar peptide (WALP23 in DMPC) where a comparison with independent results from complementary experimental methods had been possible (Holt et al. 2010; Holt et al. 2009).

All in all, for this highly mobile transmembrane helix WLP23, both the *dyn*-GALA and *dyn*-PISA implementations give the most plausible results. Both of them lead to a consistent solution for the tilt angle ($\sim$21–24°), and they yield a large width for the ρ distribution, namely $\sigma_\rho = 107°$ and 80° for *dyn*-PISA and *dyn*-GALA, respectively. Interestingly, even the rmsd maps from the two methods show comparable dependencies on τ and σ_ρ, with similarly shaped minimal rmsd regions, as illustrated in Fig. 2a, b.

To elucidate further how sensitive the two NMR approaches are towards errors in the determination of peptide orientation and dynamics, we re-analyzed another set of literature data on a related peptide (GWALP23), on the same footing (for results see Table 2). Compared with WLP23 in DMPC, the second system of GWALP23 in DLPC exhibits significantly lower mobility. Qualitatively, this lower mobility can be deduced directly from the fact that the PISEMA signals of GWALP23 are well resolved and produce a wider wheel than WLP23 (the peak positions are reproduced in Fig. 1c). The low mobility of GWALP23 had been noted before, namely in a comparison with WALP23 using fitted values of S_{zz} in a GALA analysis (Vostrikov et al. 2010). It was attributed to the presence of a single Trp residue at each end of the GWALP23 helix, as opposed to two consecutive Trp side-chains at each end in WALP23 (which is also the case of WLP23). High mobility of doubly Trp-anchored WALP/WLP peptides had also been concluded from a free energy analysis as a function of peptide orientation (Esteban-Martín et al. 2009b). When fitting the GWALP23 PISEMA data (Fig. 1c), we observed good agreement (for the center and size of the wheel) only with the *dyn*-PISA model but not with a static model, as in the case of WLP23 (Fig. 1a). This finding is in contrast to a previous study by Vostrikov et al. (2008), where a conventional (static) analysis of the PISEMA spectrum had been deemed sufficient to fit the data. This discrepancy might be explained by the reduced ^{15}N chemical shift anisotropy (CSA) tensor values used by Vostrikov et al. (2008), which apparently cause an effect similar to dynamic averaging.

When using a static GALA model to analyze GWALP23 data (Vostrikov et al. 2008), we find a reasonable fit for the ^{2}H-NMR splittings (rmsd = 0.92 kHz), though there is an improvement with the use of *dyn*-GALA (rmsd = 0.62 kHz). The static analysis again underestimates the tilt angle slightly and gives $\tau = 13°$ compared with $\tau = 18°$

from the proper dynamical analysis, but the difference is not as large as for the case of the highly mobile WLP23 (Table 2; Fig. 1d). The resulting σ_ρ distribution shows that, as already anticipated from qualitative inspection of the PISEMA spectra, GWALP23 is indeed less dynamic than WLP23 (with σ_ρ being 30–35° smaller, Table 2). Table 2 confirms that, for the moderately mobile GWALP23 in DLPC, the *dyn*-PISA and *dyn*-GALA analyses yield rather similar values for τ and σ_ρ, as was also the case for WLP23. The agreement of the two methods is in line with a previous comparison of the same peptide/lipid system using PISA and GALA, which, however, had been based on static models (Vostrikov et al. 2008) or (in the case of GALA) had considered a generalized molecular order parameter S_{zz} (Vostrikov et al. 2010). Furthermore, we find, as in the case of WLP23, that the rmsd plots from both methods also show comparable dependencies on τ and σ_ρ (Fig. 2c, d).

Conclusions

We have compared the two most widely used NMR methods for determining peptide orientation in membranes, ^{2}H-NMR and ^{15}N-PISEMA. Both approaches can yield reliable helix tilt angles and can distinguish different degrees of mobility in transmembrane peptides. However, each method suffers from different limitations, which are amplified with increasing peptide dynamics. In cases of moderate mobility (GWALP23 in DLPC), both methods give very similar results which are mildly dependent on consideration of dynamics, with only a small underestimation of the tilt when using static (or quasistatic) GALA. On the other hand, high mobility of the peptide (WLP23 in DMPC) affects both types of strategy in important and yet different ways. In the PISA approach, a static model without proper consideration of dynamics is unable to fit the data. Furthermore, large rotational fluctuations lead to severe shrinkage of the PISA wheel, and eventually to lack of signal resolution, so that the ρ angle can no longer be determined. Nevertheless, the helix tilt can still be safely deduced from the position of the center of the PISEMA signals. In contrast, the ^{2}H-NMR data (GALA analysis) can be fitted within experimental error either with or without dynamics, i.e., without noticing any serious deviations. Hence, the presence of extensive peptide dynamics cannot be deduced from these ^{2}H-NMR data alone. Therefore, as a note of caution, it is recommended that the dynamic implementation of GALA, i.e., the *dyn*-GALA approach, be chosen in all cases, to avoid underestimation of the helix tilt angle. An advantage of the GALA approach over PISA, on the other hand, is the fact that extensive dynamics do not affect the determination of ρ. We may thus summarize that *dyn*-GALA is ideally suited for determining both τ and ρ, whereas the PISEMA approach is optimally safe for finding τ alone, even from a collapsed PISA wheel and without the need to consider dynamics. These purely analytical arguments obviously do not take into account any of the advantages and disadvantages of producing ^{2}H-labeled synthetic peptides or ^{15}N-labeled material, which can be done recombinantly.

Regarding their sensitivity for determination of τ and σ_ρ, the two NMR methods may have been expected to perform differently, due to the different orientation of the respective interaction tensors in ^{2}H-NMR and ^{15}N-NMR with respect to the helix axis. However, in the representative transmembrane peptides studied here, we found that both methods are similarly capable of determining τ and σ_ρ, provided that dynamics are included.

Acknowledgments This study was supported by the DFG Center for Functional Nanostructures CFN (E1.2) and the Spanish MICINN BFU2010-19118/BMC, financed in part by the European Regional Development Fund.

References

Afonin S, Grage SL, Ieronimo M, Parvesh W, Ulrich AS (2008) Temperature-dependent transmembrane insertion of the amphiphilic peptide PGLa in lipid bilayers, observed by solid state ^{19}F NMR spectroscopy. J Am Chem Soc 130:16512–16514

Cornell BA, Separovic F, Baldassi AJ, Smith R (1988) Conformation and orientation of gramicidin A in oriented phospholipid bilayers measured by solid state carbon-13 NMR. Biophys J 53:67–76

Esteban-Martín S, Salgado J (2007) The dynamic orientation of membrane-bound peptides: bridging simulations and experiments. Biophys J 93:4278–4288

Esteban-Martín S, Strandberg E, Fuertes G, Ulrich AS, Salgado J (2009a) Influence of whole-body dynamics on ^{15}N PISEMA NMR spectra of membrane peptides: a theoretical analysis. Biophys J 96:3233–3241

Esteban-Martín S, Giménez D, Fuertes G, Salgado J (2009b) Orientational landscapes of peptides in membranes: prediction of ^{2}H NMR couplings in a dynamic context. Biochemistry 48:11441–11448

Esteban-Martín S, Strandberg E, Salgado J, Ulrich AS (2010) Solid state NMR analysis of peptides in membranes: influence of dynamics and labeling scheme. Biochim Biophys Acta 1798:252–257

Grage SL, Afonin S, Ulrich AS (2010) Dynamic transitions of membrane active peptides. Methods Mol Biol 618:183–207

Holt A, Koehorst RBM, Rutters-Meijneke T, Gelb MH, Rijkers DTS, Hemminga MA, Killian JA (2009) Tilt and rotation angles of a transmembrane model peptide as studied by fluorescence spectroscopy. Biophys J 97:2258–2266

Holt A, Rougier L, Reat V, Jolibois F, Saurel O, Czaplicki J, Killian JA, Milon A (2010) Order parameters of a transmembrane helix in a fluid bilayer: case study of a WALP peptide. Biophys J 98:1864–1872

Im W, Brooks CL III (2005) Interfacial folding and membrane insertion of designed peptides studied by molecular dynamics simulations. Proc Natl Acad Sci USA 102:6771–6776

Jo S, Im W (2011) Transmembrane helix orientation and dynamics: insights from ensemble dynamics with solid-state NMR observables. Biophys J 100:2913–2921

Killian JA, Salemink I, de Planque MR, Lindblom G, Koeppe RE II, Greathouse DV (1996) Induction of nonbilayer structures in diacylphosphatidylcholine model membranes by transmembrane α-helical peptides: importance of hydrophobic mismatch and proposed role of tryptophans. Biochemistry 35:1037–1104

Kim T, Jo S, Im W (2011) Solid-state NMR ensemble dynamics as a mediator between experiment and simulation. Biophys J 100: 2922–2928

Lee DK, Wei Y, Ramamoorthy A (2001) A two dimensional magic-angle decoupling and magic-angle turning solid-state NMR method: an application to study chemical shift tensors from peptides that are nonselectively labeled with ^{15}N isotope. J Phys Chem B 105:4752–4762

Marassi FM, Opella SJ (2000) A solid-state NMR index of membrane protein structure and topology. J Magn Reson 144:156–161

Monticelli L, Tieleman DP, Fuchs PFJ (2010) Interpretation of ^{2}H-NMR experiments on the orientation of the transmembrane helix WALP23 by computer simulations. Biophys J 99:1455–1464

Nevzorov AA, Opella SJ (2007) Selective averaging for high-resolution solid-state NMR spectroscopy of aligned samples. J Magn Reson 185:59–70

Özdirekcan S, Rijkers DTS, Liskamp RM, Killian JA (2005) Influence of flanking residues on tilt and rotation angles of transmembrane peptides in lipid bilayers. A solid-state ^{2}H NMR study. Biochemistry 44:1004–1012

Özdirekcan S, Etchebest C, Killian JA, Fuchs PF (2007) On the orientation of a designed transmembrane peptide: toward the right tilt angle? J Am Chem Soc 129:15174–15181

Separovic F, Pax R, Cornell B (1993) NMR order parameter analysis of a peptide plane aligned in a lyotropic liquid crystal. Mol Phys 78:357–369

Smith R, Separovic F, Milne TJ, Whittaker A, Bennett FM, Cornell BA, Makriyannis A (1994) Structure and orientation of the pore-forming peptide melittin, in lipid bilayers. J Mol Biol 241: 456–466

Strandberg E, Özdirekcan S, Rijkers DTS, van der Wel PCA, Koeppe RE II, Liskamp RM, Killian JA (2004) Tilt angles of transmembrane model peptides in oriented and non-oriented lipid bilayers as determined by ^{2}H solid state NMR. Biophys J 86:3709–3721

Strandberg E, Tremouilhac P, Wadhwani P, Ulrich AS (2009a) Synergistic transmembrane insertion of the heterodimeric PGLa/magainin 2 complex studied by solid-state NMR. Biochim Biophys Acta 1788:1667–1679

Strandberg E, Esteban-Martín S, Salgado J, Ulrich AS (2009b) Orientation and dynamics of peptides in membranes calculated from ^{2}H-NMR data. Biophys J 96:3223–3232

Strandberg E, Esteban-Martín S, Ulrich AS, Salgado J (2012) Hydrophobic mismatch of mobile transmembrane helices: Merging theory and experiments, Biochim Biophys Acta 1818: 1242–1249

van der Wel PCA, Strandberg E, Killian JA, Koeppe RE II (2002) Geometry and intrinsic tilt of a tryptophan-anchored transmembrane α-helix determined by ^{2}H NMR. Biophys J 83:1479–1488

Vostrikov VV, Grant CV, Daily AE, Opella SJ, Koeppe RE II (2008) Comparison of "polarization inversion with spin exchange at magic angle" and "geometric analysis of labeled alanines" methods for transmembrane helix alignment. J Am Chem Soc 130: 12584–12585

Vostrikov VV, Daily AE, Greathouse DV, Koeppe RE II (2010) Charged or aromatic anchor residue dependence of transmembrane peptide tilt. J Biol Chem 285:31723–31730

Walther TH, Grage SL, Roth N, Ulrich AS (2010) Membrane alignment of the pore-forming component $TatA_d$ of the twin-arginine translocase from *Bacillus subtilis* resolved by solid-state NMR spectroscopy. J Am Chem Soc 132:15945–15956

Wang J, Denny J, Tian C, Kim S, Mo Y, Kovacs F, Song Z, Nishimura K, Gan Z, Fu R, Quine JR, Cross TA (2000) Imaging membrane protein helical wheels. J Magn Reson 144:162–167

Wu CH, Ramamoorthy A, Opella SJ (1994) High-resolution heteronuclear dipolar solid-state NMR-spectroscopy. J Magn Reson A 109:270–272